Journal of Alloys and Compounds 696 (2017) 627–631

Contents lists available at ScienceDirect

Journal of Alloys and Compounds

journal homepage: http://www.elsevier.com/locate/jalcom

# Enhanced $^3H_4$-$^3F_4$ nonradiative relaxation of $Tm^{3+}$ through energy transfer to $Yb^{3+}$ and efficient back transfer in lowly $Tm^{3+}$ doped $Lu_{1.6}Sc_{0.4}O_3$:$Tm^{3+}$, $Yb^{3+}$

Wen Liu [a, b], Zhendong Hao [a, *], Liangliang Zhang [a], Xia Zhang [a], Yongshi Luo [a], Guohui Pan [a], Huajun Wu [a], Jiahua Zhang [a, **]

[a] State Key Laboratory of Luminescence and Applications, Changchun Institute of Optics, Fine Mechanics and Physics, Chinese Academy of Sciences, 3888 Eastern South Lake Road, Changchun, 130033, China
[b] University of Chinese Academy of Sciences, Beijing, 100049, China

ARTICLE INFO

*Article history:*
Received 23 August 2016
Received in revised form
7 November 2016
Accepted 9 November 2016
Available online 10 November 2016

*Keywords:*
Energy transfer
Thulium-ytterbium system
Radiative lifetime

ABSTRACT

Under 808 nm excitation into the $Tm^{3+}$:$^3H_4$ level, a considerable enhancement in intensity of $Tm^{3+}$: $^3F_4 \rightarrow {}^3H_6$ emission with respect to $Tm^{3+}$: $^3H_4 \rightarrow {}^3F_4$ emission is observed in $Tm^{3+}$/$Yb^{3+}$ codoped $Lu_{1.6}Sc_{0.4}O_3$. The $Tm^{3+}$-$Yb^{3+}$-$Tm^{3+}$ forward-backward energy transfer is proved to generate an additional route for the $^3H_4 \rightarrow {}^3F_4$ nonradiative relaxation, that is, energy transfer from $Tm^{3+}$:$^3H_4$ to $Yb^{3+}$:$^2F_{5/2}$ and the subsequent back transfer from $Yb^{3+}$:$^2F_{5/2}$ to $Tm^{3+}$:$^3F_4$. The analysis of emission spectra reveals that back transfer from $Yb^{3+}$ that excited by the forward energy transfer is more efficient than by absorption of 980 nm infrared light. The efficiency can reach as high as 96% with an extremely low $Tm^{3+}$ concentration (0.05%). We propose that those $Yb^{3+}$ ions with nearby $Tm^{3+}$ ions in the forward energy transfer are preferentially excited instead of equally excited as by absorption of light. The efficiencies of the energy back transfer at different $Yb^{3+}$ concentrations are evaluated, indicating that the forward-backward energy transfer can act as a dominant route for the $Tm^{3+}$: $^3H_4 \rightarrow {}^3F_4$ nonradiative relaxation when $Yb^{3+}$ concentration is higher than 5%. A method to determine the radiative rate of $Tm^{3+}$:$^3H_4$ state based on the model of cross relaxation is also demonstrated.



## 1. Introduction

$Tm^{3+}$-$Yb^{3+}$ codoped system can exhibit strong $Tm^{3+}$ blue upconversion luminescence under near infrared (NIR) excitation, as well as under red light excitation [1–3]. The blue emitting level $^1G_4$ of $Tm^{3+}$ can be populated either from $Tm^{3+}$:$^3H_4$ by energy transfer from $Yb^{3+}$ under NIR excitation [4,5] or from $Tm^{3+}$:$^3F_4$ by absorbing a red photon under red light excitation [6]. Hence, the relaxation rate from $^3H_4$ to $^3F_4$ state influences the blue emission intensities for both NIR and red excitations. Obviously, improving this relaxation is conductive to the blue upconversion luminescence under red light excitation. G. Özen et al. observed a remarkable enhancement in the blue emission upon red light excitation at 683 nm in $Tm^{3+}$/$Yb^{3+}$ codoped fluorophosphate glasses compared with $Tm^{3+}$ singly doped counterpart [2]. The mechanism for the enhancement was revealed to result from the enhanced $^3H_4$-$^3F_4$ nonradiative relaxation through $Tm^{3+}$-$Yb^{3+}$-$Tm^{3+}$ forward-backward energy transfer (FBET) [7]. The same phenomenon that efficient backward energy transfer (BET) increase the Tm:$^3F_4$ level population has also been reported recently [8]. While, the efficiency of BET may be valued inappropriately in previous studies. The efficiency of BET was simply regarded as energy transfer efficiency from donor ($Yb^{3+}$) to acceptor ($Tm^{3+}$, $Nd^{3+}$, $Er^{3+}$, etc.) after $Yb^{3+}$ direct excitation [2,9–11]. In the $Tm^{3+}$-$Yb^{3+}$-$Tm^{3+}$ FBET, however, $Yb^{3+}$ ions functioned in BET are mainly excited by FET from $Tm^{3+}$. It is, therefore, speculated that the $Yb^{3+}$ with a nearby $Tm^{3+}$ is preferentially excited in the FET rather than equally excited by direct absorption of light. In this situation, the efficient BET is expected for the close-ranged $Yb^{3+}$-$Tm^{3+}$ pairs selected by the FET. However, the efficient BET due to the selective excitation of $Yb^{3+}$ by the FET has not been studied. It is reported lately that the BET could also contribute to the enhancement in the $Tm^{3+}$ 1.8 μm emission

* Corresponding author.
** Corresponding author.
*E-mail addresses:* haozhendong0451@yahoo.cn (Z. Hao), zhangjh@ciomp.ac.cn (J. Zhang).

http://dx.doi.org/10.1016/j.jallcom.2016.11.126
0925-8388/

when co-doped with $Yb^{3+}$ [12]. Consequently, evaluating the backward transfer efficiency in $Tm^{3+}$-$Yb^{3+}$-$Tm^{3+}$ FBET is necessary for quantitatively understanding the enhanced $^3H_4$-$^3F_4$ nonradiative relaxation involved in many luminescence processes of $Tm^{3+}$ and $Yb^{3+}$ codoped systems [13]. In our previous work, considerably enhanced nonradiative relaxation of $Er^{3+}$:$^4S_{3/2}$-$^4F_{9/2}$ by $Er^{3+}$-$Yb^{3+}$-$Er^{3+}$ FBET was observed in $Er^{3+}$ and $Yb^{3+}$ codoped $Y_2O_3$ and $NaYF_4$ host [14,15]. The FBET includes a cross relaxation [16] from $Er^{3+}$:$^4S_{3/2}$ to $Yb^{3+}$:$^2F_{5/2}$ followed by $Er^{3+}$ depopulation down to the $^4I_{13/2}$ and the energy back transfer from the excited $Yb^{3+}$ that populates $Er^{3+}$ from $^4I_{13/2}$ to $^4F_{9/2}$.

In this paper, the enhanced $^3H_4$-$^3F_4$ nonradiative relaxation of $Tm^{3+}$ through $Tm^{3+}$-$Yb^{3+}$-$Tm^{3+}$ FBET is observed in $Tm^{3+}$ and $Yb^{3+}$ codoped $Lu_{1.6}Sc_{0.4}O_3$. We report, for the first time, the effect of preferential excitation of $Yb^{3+}$ with a nearby $Tm^{3+}$ in the FET that can result in an efficient BET to $Tm^{3+}$ even if the $Tm^{3+}$ concentration is as low as 0.05%. Furthermore, we find efficient BET makes the FBET to be a dominant route for populating $Tm^{3+}$:$^3F_4$ from $Tm^{3+}$:$^3H_4$ when $Yb^{3+}$ concentration is higher than 5%.

## 2. Experimental

### 2.1. Sample preparation

The synthesis of $(Lu_{0.8}Sc_{0.2})_2O_3$: 0.0005 $Tm^{3+}$/x$Yb^{3+}$(0, 0.02, 0.05, 0.1) powder samples $(Lu_{0.8-0.0005-x}Sc_{0.2}Tm_{0.0005}Yb_x)_2O_3$ by the urea homogeneous precipitation method was described as follows: the appropriate amounts of $Lu_2O_3$ (4N), $Sc_2O_3$ (4N), $Tm_2O_3$ (4N) and $Yb_2O_3$ (4N) powders were dissolved in nitric acid respectively to obtain 0.1M $Lu(NO_3)_3$, 0.1M $Sc(NO_3)_3$, 0.1M $Yb(NO_3)_3$ and 0.004M $Tm(NO_3)_3$ solutions. The constant stoichiometric molarity of the $Sc^{3+}$ and $Lu^{3+}$ stock solutions was maintained as 1:4 for all the starting solutions. Next, the aqueous solutions containing $Lu^{3+}$, $Sc^{3+}$, $Tm^{3+}$/$Yb^{3+}$ and urea with corresponding mole ratios were mixed to acquire homogeneous solutions and then heated to 90 °C with continuous stirring. After holding the temperature for 1.5 h, the solutions were cooled down naturally. The precipitates were separated from the supernatant materials via centrifugation at high speed of 8000r/min. Afterwards the powders were washed four times with deionized water and absolute ethanol and then dried in a vacuum desiccator at 60 °C for 24 h. The samples were obtained after being calcined at 1500 °C for 4 h in air.

For comparison, the sample of $(Lu_{0.8}Sc_{0.2})_2O_3$: 0.005 $Tm^{3+}$ was also prepared via the above-mentioned procedure to calculate the radiative lifetime together with the $(Lu_{0.8}Sc_{0.2})_2O_3$: 0.0005 $Tm^{3+}$ sample. In this work, experiments were conducted at low concentrations of $Tm^{3+}$ to avoid the interaction among $Tm^{3+}$ ions, so that the forward-backward energy transfer process could be simplified [17].

### 2.2. Spectroscopy measurements

The steady state emission spectra were measured using an FLS920 spectrometer (Edinburgh Instruments, U.K.). An 808 nm laser diode (LD) was used to excite $Tm^{3+}$:$^3H_4$ level and a 980 nm LD to excite $Yb^{3+}$:$^2F_{5/2}$ level. In energy level lifetime measurements, a 10 ns pulsed laser with tunable wavelengths from an optical parametric oscillator (OPO) pumped by a Nd:YAG laser (spectra-physics, GCR 130) was used as an excitation source. The excitation wavelength was tuned to 685 nm to excite $Tm^{3+}$:$^3F_2$, which rapidly relaxes down to the $Tm^{3+}$:$^3H_4$, for $^3H_4$ lifetime measurement. The signals were detected by a Tektronix digital oscilloscope (TDS 3052). The lifetimes were defined as the integration of the area under the corresponding decay curves with normalized initial intensity. All of the measurements above were performed at room temperature.

## 3. Results and discussion

### 3.1. Observation of efficient BET in $Tm^{3+}$-$Yb^{3+}$-$Tm^{3+}$ FBET

Fig. 1 shows the emission spectra of $(Lu_{0.8}Sc_{0.2})_2O_3$: 0.05% $Tm^{3+}$, x%$Yb^{3+}$ (x = 0, 2, 5, 10) upon $Tm^{3+}$: $^3H_4$ excitation at 808 nm (black line and red dotted line) and upon $Yb^{3+}$: $^2F_{5/2}$ excitation at 980 nm (blue line). The emission peaked at around 1030 nm is originated from $Yb^{3+}$:$^2F_{5/2}$ → $^2F_{7/2}$ transition. The group of emission lines in the range of 1300–1600 nm is responsible for $Tm^{3+}$: $^3H_4$→$^3F_4$ transition. The band peaked at 1620 nm is a part of $Tm^{3+}$: $^3F_4$→$^3H_6$ emissions which in fact have the strongest peak around 2 μm. The wavelength longer than 1620 nm is undetected because of a cutoff wavelength at 1650 nm by the InGaAs detector used in the present work. For clear comparison the emission spectrum of each codoped sample (black line) and $Tm^{3+}$ singly doped sample (red dotted line) are plotted together, where the $^3H_4$→$^3F_4$ emission intensity for the singly doped sample is scaled to that for the codoped sample. Meanwhile, the $Yb^{3+}$ emission intensity in each codoped sample upon 980 nm excitation is scaled to that upon 808 nm excitation.

In Fig. 1, the appearance of $Yb^{3+}$ emission upon $Tm^{3+}$: $^3H_4$ excitation is a direct evidence for the forward energy transfer from $Tm^{3+}$: $^3H_4$ to $Yb^{3+}$: $^2F_{5/2}$. Besides that the $^3F_4$→$^3H_6$ emission

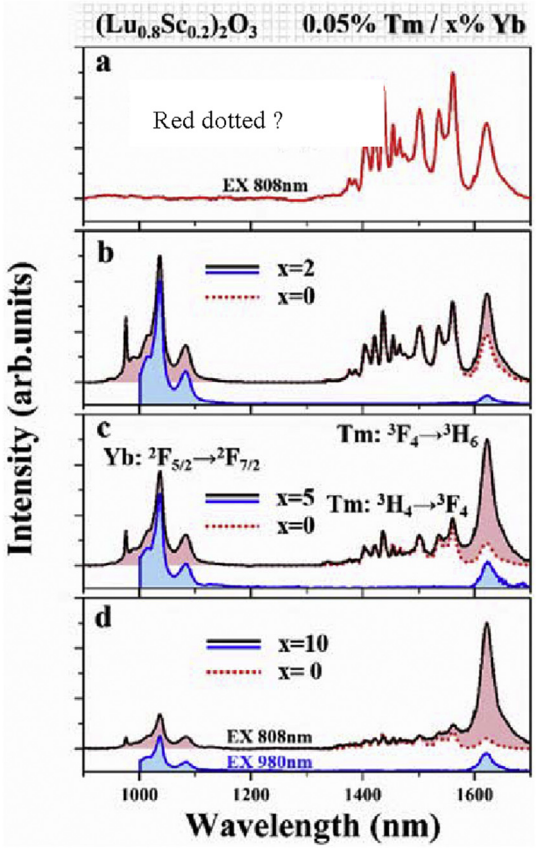


**Fig. 1.** NIR emission spectra of samples $(Lu_{0.8}Sc_{0.2})_2O_3$: 0.05%$Tm^{3+}$/x %$Yb^{3+}$ (x = 0, 2, 5, 10) upon $Tm^{3+}$: $^3H_4$ excitation at 808 nm (red dotted for x = 0, and black solid for x > 0 with the maximum emission intensity normalized). The $^3H_4$→$^3F_4$ emission intensity for $Tm^{3+}$ singly doped sample is scaled to that for the codoped sample. The emission spectra upon $Yb^{3+}$ excitation at 980 nm are also plotted (blue solid) with the $Yb^{3+}$ emission intensities are scaled to that upon 808 nm excitation. (For interpretation of the references to colour in this figure legend, the reader is referred to the web version of this article.)

intensity for each codoped samples is always stronger than that for the singly doped sample upon $Tm^{3+}$: $^3H_4$ excitation and the increment (red shaded in the $^3F_4 \rightarrow {}^3H_6$ emission) becomes larger with the increase of $Yb^{3+}$ concentration.

Upon $Tm^{3+}$: $^3H_4$ excitation for $Tm^{3+}$ singly doped sample, the $^3F_4$ level is populated by the intrinsic $^3H_4$-$^3F_4$ relaxation and the cross relaxation (CR) between $Tm^{3+}$ ions described as ($^3H_4 \rightarrow {}^3F_4$)-($^3H_6 \rightarrow {}^3F_4$) [18]. In case of low $Tm^{3+}$ concentration of 0.05% in the present work, the CR can be neglected. The intrinsic $^3H_4$-$^3F_4$ relaxation includes $^3H_4 \rightarrow {}^3F_4$, $^3H_5$ radiative transitions and the cascade MPR through $^3H_5$. If the MPR and radiative rates are independent on $Yb^{3+}$ concentration, the increments in the $^3F_4 \rightarrow {}^3H_6$ emission intensity for the co-doped samples indicate the effect of the $Tm^{3+}$ -$Yb^{3+}$ -$Tm^{3+}$ FBET, as sketched in Fig. 2.

Alternatively, the energy back transfer from $Yb^{3+}$ to $Tm^{3+}$ is also observed as $Yb^{3+}$ is directly excited at 980 nm, showing $Tm^{3+}$ emission (blue shaded) as well as $Yb^{3+}$ emission. We notice that the $Tm^{3+}$: $^3F_4 \rightarrow {}^3H_6$ emission intensity increment (red shaded) upon $Tm^{3+}$: $^3H_4$ excitation (808 nm) is more stronger than the $Tm^{3+}$: $^3F_4 \rightarrow {}^3H_6$ emission intensity (blue shaded) upon 980 nm excitation for each codoped sample when the $Yb^{3+}$ emissions for the two excitation conditions are normalized in intensity. From Fig. 1, the $^3F_4 \rightarrow {}^3H_6$ emission intensity ratios of the red shaded to the blue shaded area are 5.3, 4.2 and 6.3 for $Yb^{3+}$ concentration of 2%, 5% and 10%, respectively. As a result, the BET from $Yb^{3+}$ to $Tm^{3+}$ upon 808 nm excitation is more efficient than upon 980 nm excitation. Because the doped $Tm^{3+}$ and $Yb^{3+}$ ions follow a random distribution model based on space homogeneous distribution in the host, random distances between $Tm^{3+}$ and $Yb^{3+}$ ions could be expected. Therefore, we attribute this result to the preferential excitation of $Yb^{3+}$ with a nearby $Tm^{3+}$ ion in the step of FET from $Tm^{3+}$ upon 808 nm excitation. At low doping level of $Tm^{3+}$ (0.05%) in this work, a nearby $Tm^{3+}$ ion around a $Yb^{3+}$ ion can act as a dominant acceptor in BET from the $Yb^{3+}$ because the $Tm^{3+}$ ions are thin. Naturally, we can observe a remarkable enhancement of BET upon 808 nm excitation than upon 980 nm excitation. In contrast, high $Tm^{3+}$ concentration could make a less enhancement because the dense $Tm^{3+}$ ions may act as the dominant acceptors rather than a nearby $Tm^{3+}$ in the BET from $Yb^{3+}$. In essence, energy transfer process is greatly affected by transfer from first and second-neighbor coordinations in oxides which could facilitate the transfer process [19]. While, it is on the condition that the amounts of ions at close and long range are in the same order of magnitude. If the density of long-range ions is high enough, the overall transfer effect by long-range ions makes the BET not obvious. Therefore, when discussing about the relationship between the BET and the concentration, it should be noted that the efficient BET is prominent at low concentration level.

### 3.2. Energy transfer efficiencies

In the presence of FBET in the codoped samples upon $Tm^{3+}$:$^3H_4$ excitation, the $Tm^{3+}$:$^3F_4 \rightarrow {}^3H_6$ emission can be divided into two parts. One is contributed by FBET, responsible for the red shaded intensity in the $^3F_4 \rightarrow {}^3H_6$ emission, here denoted by $\Delta I$. The left part (red dotted) is contributed by the intrinsic $^3H_4$-$^3F_4$ relaxation, here denoted by $I_0$. $\Delta I$ should be proportional to $\eta_{FET}\eta_{BET}$, where $\eta_{FET}$ and $\eta_{BET}$ are efficiencies of FET and BET, respectively. $I_0$ should be proportional to $\theta(1-\eta_{FET})$, where $\theta$ is a ratio of the intrinsic $^3H_4$-$^3F_4$ relaxation rate to the total intrinsic decay rate of $^3H_4$ for $Tm^{3+}$ singly doped sample at low concentration. Thus, we have

$$\frac{\Delta I}{I_0} = \frac{\eta_{FET}\eta_{BET}}{\theta(1-\eta_{FET})} \quad (1)$$

To obtain the efficiency of FET, the decay curves of $Tm^{3+}$: $^3H_4 \rightarrow {}^3H_6$ emission for different $Yb^{3+}$ concentrations are measured, as displayed in Fig. 3. $\eta_{FET}$ can be calculated by Ref. [20].

$$\eta_{FET} = 1 - \tau_0^{-1} \int_0^{\infty} I(t)dt \quad (2)$$

where $\tau_0$ is the intrinsic lifetime of $Tm^{3+}$:$^3H_4$, obtained from the sample with singly and low (0.05%) doped $Tm^{3+}$ in this work. $I(t)$ is the fluorescence decay function of $Tm^{3+}$:$^3H_4$ with $I(0) = 1$.

In Eq. (1), $\Delta I/I_0$ can be drawn from the emission spectra in Fig. 1, $\eta_{FET}$ is figured out using Eq. (2) based on the decay curves shown in Fig. 3. $\theta$ is determined to be 0.39 based on CR analysis that will be presented in the next section. The values of $\eta_{BET}$ are obtained as listed in Table 1. The efficiency of the FBET is calculated by $\eta_{FBET} = \eta_{FET}\eta_{BET}$ and the intrinsic $^3H_4$-$^3F_4$ relaxation is calculated by $\eta_{INR} = \theta(1-\eta_{FET})$.

As exhibited in Table 1, a marked increase in $\eta_{FET}$, $\eta_{BET}$, $\eta_{FBET}$ and a rapid decrease in $\eta_{INR}$ have been observed with increasing the $Yb^{3+}$ doping level. The backward efficiency can reach 96% for $Yb^{3+}$ concentration of 5% although the concentration of $Tm^{3+}$ as the

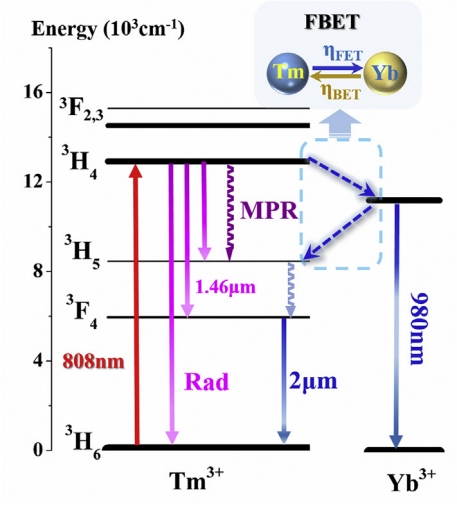


**Fig. 2.** Thulium-ytterbium energy level diagram under 808 nm excitation. The dashed arrows correspond to the forward-backward energy transfer process.

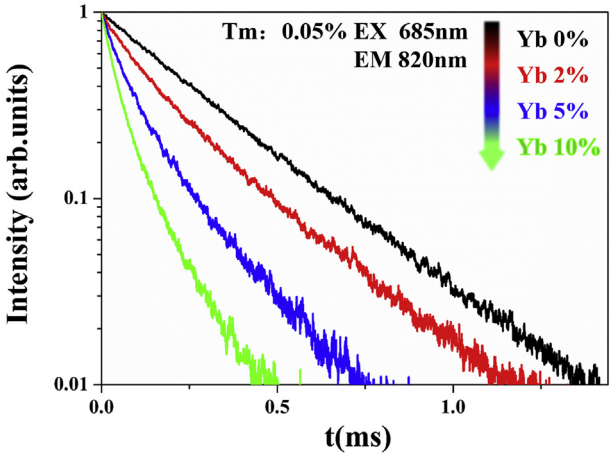


**Fig. 3.** Decay curves of $Tm^{3+}$: $^3H_4$ level in $(Lu_{0.8}Sc_{0.2})_2O_3$: 0.05mol%$Tm^{3+}$/xmol%$Yb^{3+}$ (x = 0, 2, 5, 10).

**Table 1**
Efficiencies of energy transfers and the intrinsic $^3H_4$-$^3F_4$ relaxation in $(Lu_{0.8}Sc_{0.2})_2O_3$: 0.05mol%Tm/x%Yb.

| x (%) | $\eta_{FET}$ | $\eta_{BET}$ | $\eta_{FBET}$ | $\eta_{INR}$ |
|---|---|---|---|---|
| 0 | 0 | – | 0 | 0.39 |
| 2 | 0.32 | 0.70 | 0.22 | 0.26 |
| 5 | 0.65 | 0.96 | 0.62 | 0.14 |
| 10 | 0.84 | 0.68 | 0.57 | 0.06 |

acceptor in the BET is as low as 0.05%, reflecting the effect of the preferential excitation of $Yb^{3+}$ with a nearby $Tm^{3+}$ ion in the step of FET. The FBET offers an additional route for relaxation from $Tm^{3+}$:$^3H_4$ down to $Tm^{3+}$:$^3F_4$ through $Yb^{3+}$ as an intermediate ion and this route is more effective than the intrinsic $^3H_4$-$^3F_4$ relaxation as $Yb^{3+}$ concentration higher than 0.05 with a fixed $Tm^{3+}$ concentration as low as 0.0005.

Notably, as Table 1 presented, with the increase of $Yb^{3+}$ concentration the $\eta_{BET}$ increases firstly and then shows a decline when $Yb^{3+}$ concentration over 5%. This result is explained as follows: under 808 nm excitation, $Tm^{3+}$:$^3H_4$ is populated firstly. Subsequently, the excited $Tm^{3+}$ may transfer energy to the nearest $Yb^{3+}$ or other $Yb^{3+}$ outside the nearest shell. With the increase of $Yb^{3+}$ concentration, the fraction of the excited $Yb^{3+}$ ions that is located in the nearest site of $Tm^{3+}$ increases. Hence, the energy back transfer becomes more efficient. As the $Yb^{3+}$ concentration is further raised, for instance higher than 5%, energy transfer between $Yb^{3+}$ ions begins to get very competitive that may reduce the efficiency of energy back transfer from $Yb^{3+}$ to $Tm^{3+}$ [21].

### 3.3. Determination of θ value

We determine the θ value basing on analysis of the effect of cross relaxation process on the emission spectrum for 0.5% $Tm^{3+}$ singly doped sample. The CR process between two $Tm^{3+}$ ions is presented in Fig. 4. As the $^3H_4$ level is populated, the CR can convert one $Tm^{3+}$ ion in the $^3H_4$ state into two $Tm^{3+}$ ions in the $^3F_4$ state. Fig. 5 shows the emission spectra of $Tm^{3+}$ single doped $(Lu_{0.8}Sc_{0.2})_2O_3$: 0.05mol % Tm and $(Lu_{0.8}Sc_{0.2})_2O_3$: 0.5mol%Tm samples upon $^3H_4$ excitation. The spectra are scaled on the $^3H_4 \rightarrow {}^3F_4$ emission intensity. When the doping level is low enough (0.05mol%), the CR can be neglected and the $^3F_4 \rightarrow {}^3H_6$ emission is mainly populated by the intrinsic

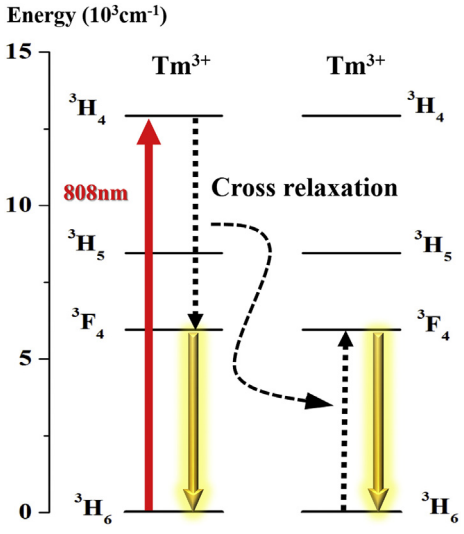


**Fig. 4.** Energy level diagram with the CR processes between $Tm^{3+}$ ions following 808 nm excitation.

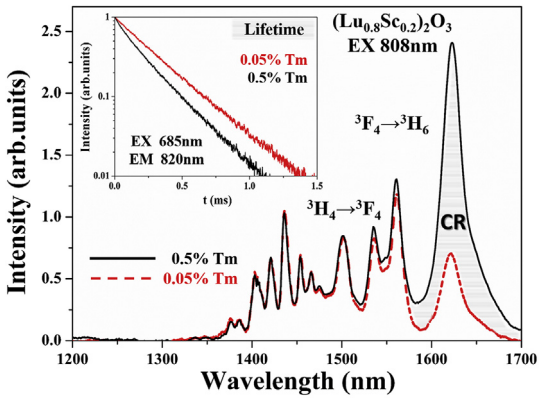


**Fig. 5.** The infrared emission spectra of $(Lu_{0.8}Sc_{0.2})_2O_3$: 0.05mol%Tm and $(Lu_{0.8}Sc_{0.2})_2O_3$: 0.5mol%Tm samples pumped under 808 nm excitation. The 1.46 μm intensities are normalized. The inset shows the fluorescence lifetimes of $Tm^{3+}$ emission (800 nm) in two samples.

$^3H_4$-$^3F_4$ relaxation. At high $Tm^{3+}$ concentration (0.5mol%), the CR is evident and it considerably enhances the $^3F_4 \rightarrow {}^3H_6$ emission intensity (shaded area). The CR has speeded up the decay of the $^3F_4 \rightarrow {}^3H_6$ transition, as demonstrated in the inset of Fig. 5. The efficiency ($\eta_{CR}$) of the CR is calculated to be 0.32 using Eq. (2). The $^3H_4$ population that survives the CR is $1-\eta_{CR}$, the fraction of which that contributes to the $^3F_4$ population is θ. Considering that the CR cuts each $^3H_4$ population into two $^3F_4$ population, we have

$$\frac{\Delta I_{CR}}{I_0} = \frac{2\eta_{CR}}{\theta(1-\eta_{CR})} \tag{3}$$

where the $I_0$ is the intensity of $^3F_4 \rightarrow {}^3H_6$ emission in the absence of CR for $Tm^{3+}$ concentration of 0.05%. $\Delta I_{CR}$ is the increment (shaded area) in $^3F_4 \rightarrow {}^3H_6$ emission intensity in the presence of CR for $Tm^{3+}$ concentration of 0.5%. From Fig. 5, $\Delta I_{CR}/I_0$ is obtained to be 2.4. Substitutions of $\Delta I_{CR}/I_0$ of 2.4 and $\eta_{CR}$ of 0.32 in Eq. (3) give θ = 0.39. In addition, the definition of θ gives

$$\theta = 1-(1-\beta)\frac{\tau_0}{\tau_r} \tag{4}$$

Where β is the sum of branch ratios of $^3H_4 \rightarrow {}^3H_5$ and $^3H_4 \rightarrow {}^3F_4$ radiative transitions, $\tau_r$ is the radiative lifetime of $^3H_4$. Substituting θ of 0.39 into Equation (4) and selecting β = 0.1 based on some previous reports [22,23], we finally obtain the $^3H_4$ radiative lifetime $\tau_r$ to be 417 μs in $Lu_{1.6}Sc_{0.4}O_3$: Tm sample. Compared with the radiative lifetimes (690 μs) of $Lu_2O_3$ calculated by J-O theory [24], our method above is also reasonable and offers a new way to calculate radiative lifetime when the absorption spectra has difficulty in measuring.

## 4. Conclusions

In summary, $Lu_{1.6}Sc_{0.4}O_3$: 0.0005 $Tm^{3+}$/x$Yb^{3+}$ (0, 0.02, 0.05, 0.1) samples have been prepared and enhanced luminescence of $Tm^{3+}$:$^3F_4 \rightarrow {}^3H_6$ have been presented in this study. This phenomenon could be attributed to the efficient $Tm^{3+}$-$Yb^{3+}$-$Tm^{3+}$ FBET. It is found that the BET to $Tm^{3+}$ from $Yb^{3+}$ excited by the FET is more efficient than by direct excitation of $Yb^{3+}$:$^2F_{5/2}$ at 980 nm. The efficiency of BET can reach 96% for $Yb^{3+}$ concentration of 5% with the concentration of $Tm^{3+}$ regarded as acceptor as low as 0.05%. Based on that, we propose that those $Yb^{3+}$ ions that have a nearby $Tm^{3+}$ ion in the FET are preferentially excited instead of equally excited such as by absorption of light, thus leading to an efficient BET to

$Tm^{3+}$ in spite of low doping level. The FBET may act as a dominant route for populating $Tm^{3+}$:$^3F_4$ from $Tm^{3+}$:$^3H_4$ rather than the intrinsic $^3H_4$-$^3F_4$ relaxation when the $Yb^{3+}$ concentration reaches 5%. The increased relaxation rate from $^3H_4$ to $^3F_4$ may contribute to enhance blue upconversion luminescence under red light excitation. In addition, a method to determine the radiative rate of $Tm^{3+}$:$^3H_4$ state based on the model of cross relaxation between $Tm^{3+}$ ions is demonstrated and the $Tm^{3+}$:$^3H_4$ radiative lifetime of 417 μs is obtained.

## Acknowledgments

This work was partially supported by the National Key R&D Program of China (Grant No. 2016YFB0701003, 2016YFB0400605), National Natural Science Foundation of China (Grant No. 61275055, 11274007, 51402284 and 11604330) and the Natural Science Foundation of Jilin Province (Grant No. 20140101169JC, 20150520022JH and 20160520171JH).

## References

[1] J.C. Boyer, F. Vetrone, L.A. Cuccia, Synthesis of colloidal upconverting $NaYF_4$ nanocrystals doped with $Er^{3+}$, $Yb^{3+}$ and $Tm^{3+}$, $Yb^{3+}$ via thermal decomposition of lanthanide trifluoroacetate precursors, J. Am. Chem. Soc. 128 (23) (2006) 7444–7445.
[2] G. Özen, J.P. Denis, P. Goldner, Enhanced $Tm^{3+}$ blue emission in Tm, Yb, co-doped fluorophosphate glasses due to back energy transfer processes, Appl. Phys. Lett. 62 (9) (1993) 928–930.
[3] G. Özen, J.P. Denis, M. Genotelle, Tm-Yb-Tm energy transfers and effect of temperature on the fluorescence intensities in oxyfluoride tellurite compounds, J. Phys. Condens. Mat. 7 (22) (1995) 4325.
[4] F.W. Ostermayer Jr., J.P. Van der Ziel, H.M. Marcos, Frequency upconversion in $YF_3$: $Yb^{3+}$, $Tm^{3+}$, Phys. Rev. B 3 (8) (1971) 2698.
[5] K. Liu, Z. Zhang, C. Shan, A flexible and superhydrophobic upconversion-luminescence-membrane as an ultrasensitive fluorescence sensor for single droplet detection, Light Sci. Appl. 5 (2016) e16136.
[6] W. Xu, J.P. Denis, G. Özen, Red to blue up-conversion emission of $Tm^{3+}$ ions in $Yb^{3+}$-doped glass ceramic, J. Appl. Phys. 75 (8) (1994) 4180–4188.
[7] L. Huang, S. Shen, A. Jha, Near infrared spectroscopic investigation of $Tm^{3+}$–$Yb^{3+}$ co-doped tellurite glasses, J. Non-Cryst. Solids 345 (2004) 349–353.
[8] R. Zhuang, D. Wen, Z. Zhuang, Red to UV and blue up-conversion in alumina sol containing only $Tm^{3+}$ or both $Tm^{3+}$ and $Yb^{3+}$ ions via low energy pumping, J. Alloys Compd. 658 (2016) 488–493.
[9] A. Bednarkiewicz, M. Stefanski, R. Tomala, Near infrared absorbing near infrared emitting highly-sensitive luminescent nanothermometer based on $Nd^{3+}$ to $Yb^{3+}$ energy transfer, Phys. Chem. Chem. Phys. 17 (37) (2015) 24315–24321.
[10] J. Liu, H. Deng, Z. Huang, Phonon-assisted energy back transfer-induced multicolor upconversion emission of $Gd_2O_3$: $Yb^{3+}$/$Er^{3+}$ nanoparticles under near-infrared excitation, Phys. Chem. Chem. Phys. 17 (23) (2015) 15412–15418.
[11] J. Zhang, S. Wang, N. Gao, Luminescence energy transfer detection of PSA in red region based on $Mn^{2+}$-enhanced $NaYF_4$: Yb, Er upconversion nanorods, Biosens. Bioelectron. 72 (2015) 282–287.
[12] S. Balaji, K. Biswas, A.D. Sontakke, Enhanced 1.8 μm emission in $Yb^{3+}$/$Tm^{3+}$ co-doped tellurite glass: effects of $Yb^{3+}$ ↔ $Tm^{3+}$ energy transfer and back transfer, J. Quant. Spectrosc. Radiat. Transf. 147 (2014) 112–120.
[13] A. Braud, S. Girard, J.L. Doualan, Energy-transfer processes in Yb: Tm-doped $KY_3F_{10}$, $LiYF_4$, and $BaY_2F_8$ single crystals for laser operation at 1.5 and 2.3 μm, Phys. Rev. B 61 (8) (2000) 5280.
[14] J. Zhang, Z. Hao, J. Li, Observation of efficient population of the red-emitting state from the green state by non-multiphonon relaxation in the $Er^{3+}$–$Yb^{3+}$ system, Light Sci. Appl. 4 (1) (2015) e239.
[15] G. Xiang, J. Zhang, Z. Hao, Importance of suppression of $Yb^{3+}$ de-excitation to upconversion enhancement in β-$NaYF_4$: $Yb^{3+}$/$Er^{3+}$@ β-NaYF4 sandwiched structure nanocrystals, Inorg. Chem. 54 (8) (2015) 3921–3928.
[16] F. Vetrone, J.C. Boyer, J.A. Capobianco, Significance of $Yb^{3+}$ concentration on the upconversion mechanisms in codoped $Y_2O_3$: $Er^{3+}$, $Yb^{3+}$ nanocrystals, J. Appl. Phys. 96 (2004) 661–667.
[17] V. Mahalingam, F. Vetrone, R. Naccache, Colloidal $Tm^{3+}$/$Yb^{3+}$-Doped LiYF4 nanocrystals: multiple luminescence spanning the UV to NIR regions via low-energy excitation, Adv. Mater. 21 (40) (2009) 4025–4028.
[18] J. Ganem, J. Crawford, P. Schmidt, Thulium cross-relaxation in a low phonon energy crystalline host, Phys. Rev. B 66 (24) (2002) 245101.
[19] G. Lakshminarayana, J. Qiu, M.G. Brik, Spectral analysis of $Er^{3+}$, $Er^{3+}$/$Yb^{3+}$and $Er^{3+}$/$Tm^{3+}$/$Yb^{3+}$ doped $TeO_2$–ZnO–$WO_3$–$TiO_2$–$Na_2O$ glasses, J. Phys. Condens. Mater. 20 (37) (2008) 375101.
[20] K. Beil, C.J. Saraceno, C. Schriber, Yb-doped mixed sesquioxides for ultrashort pulse generation in the thin disk laser setup, Appl. Phys. B Lasers. 113 (1) (2013) 13–18.
[21] G. Lakshminarayana, H. Yang, S. Ye, Co-operative downconversion luminescence in $Tm^{3+}$/$Yb^{3+}$: $SiO_2$–$Al_2O_3$–LiF–$GdF_3$ glasses, J. Phys. D. Appl. Phys. 41 (17) (2008) 175111.
[22] P.Y. Poma, K.U. Kumar, M.V.D. Vermelho, Luminescence and thermal lensing characterization of singly $Eu^{3+}$ and $Tm^{3+}$ doped $Y_2O_3$ transparent ceramics, J. Lumin 161 (2015) 306–312.
[23] C. Gheorghe, A. Lupei, V. Lupei, Intensity parameters of $Tm^{3+}$ doped $Sc_2O_3$ transparent ceramic laser material, Opt. Mater. 33 (3) (2011) 501–505.
[24] L. Fornasiero, $Nd^{3+}$ and $Tm^{3+}$-dotierte Sesquioxide, Universität Hamburg, 1999. Ph.D. thesis.